Supporting Information

High-Accuracy Vapor Pressure Data of the Extended $[C_nC_1im][Ntf_2]$ Ionic Liquid Series: Trend Changes and Structural Shifts

Marisa A. A. Rocha [†, §], *Carlos F. R. A. C. Lima* [†], *Lígia R. Gomes* [#], *Bernd Schröder* [§], *João A. P. Coutinho* [§], *Isabel M. Marrucho* [§,¥], *José M. S. S. Esperança* [¥], *Luís P. N. Rebelo* [¥] *K. Shimizu* [£], *José N. Canongia Lopes* [£], *Luís M. N. B. F. Santos* [†,*]

[†] Centro de Investigação em Química, Faculdade de Ciências da Universidade do Porto, R. Campo Alegre 687, P-4169-007 Porto, Portugal

[§] CICECO, Departamento de Química, Universidade de Aveiro, 3810-193 Aveiro, Portugal

[#] CIAGEB, Faculdade de Ciências da Saúde da UFP, Universidade Fernando Pessoa, R. Carlos da Maia 296, P-4200-150 Porto, Portugal

[¥] Instituto de Tecnologia Química e Biológica, ITQB2, Universidade Nova de Lisboa, AV. República, Apartado 127, 2780-901 Oeiras, Portugal

[£] Centro de Química Estrutural/IST, Av. Rovisco Pais 1049 001 Lisboa, Portugal

*Corresponding author. Tel.: +351 220 402 836; Fax: +351 220 402 659

E-mail address: lbsantos@fc.up.pt (Luís M. N. B. F. Santos)

Vapor pressures measurements using Quartz crystal microbalance Knudsen effusion apparatus

The experimental vapor pressures for each IL, obtained by the quartz microbalance Knudsen effusion apparatus, appear in Table S1.

Table S1 Experimental vapor pressures for the nine imidazolium based ILs, obtained by the quartz crystal microbalance Knudsen effusion apparatus.

T / K	p / Pa	Δp / Pa	T / K	p / Pa	Δp / Pa	T / K	p / Pa	Δp / Pa
				[C_2C_1im][Ntf_2]				
445.30	0.0069	-0.0001	459.32	0.0183	0.0002	473.32	0.0436	-0.0002
447.30	0.0082	0.0002	461.32	0.0208	0.0002	475.33	0.0488	-0.0007
449.31	0.0091	-0.0001	463.34	0.0235	0.0000	477.33	0.0552	-0.0006
451.31	0.0106	0.0000	465.34	0.0264	-0.0003	479.34	0.0625	-0.0004
453.31	0.0121	0.0000	467.36	0.0303	0.0000	481.34	0.0720	0.0012
455.32	0.0138	-0.0001	469.34	0.0340	-0.0003	483.41	0.0821	0.0023
457.32	0.0159	0.0001	471.35	0.0383	-0.0006			
				[C_3C_1im][Ntf_2]				
453.13	0.0147	0.0003	467.02	0.0355	-0.0002	480.98	0.0809	-0.0023
455.11	0.0167	0.0002	469.04	0.0400	-0.0005	482.98	0.0919	-0.0015
457.11	0.0190	0.0002	471.00	0.0453	-0.0004	484.98	0.1054	0.0006
459.11	0.0216	0.0001	473.04	0.0520	0.0002	486.96	0.1194	0.0021
461.08	0.0244	0.0000	475.12	0.0577	-0.0010	488.95	0.1347	0.0035
463.06	0.0276	-0.0001	477.00	0.0649	-0.0008	490.95	0.1492	0.0025
465.06	0.0313	-0.0002	478.99	0.0721	-0.0019	492.95	0.1669	0.0030
				[C_4C_1im][Ntf_2]				
463.07	0.0234	0.000	473.02	0.0447	0.000	482.95	0.0825	0.000
465.06	0.0269	0.000	475.00	0.0506	0.000	484.97	0.0942	0.001
467.06	0.0303	0.000	477.18	0.0572	-0.001	486.95	0.1051	0.000
469.05	0.0348	0.000	478.96	0.0646	0.000			
471.05	0.0394	0.000	480.96	0.0730	0.000			

				[C_5C_1im im][Ntf_2]				
457.09	0.0140	0.0001	471.03	0.0361	-0.0006	484.93	0.0901	0.0000
459.08	0.0163	0.0002	473.01	0.0414	-0.0005	486.91	0.1021	0.0002
461.06	0.0187	0.0002	475.01	0.0474	-0.0004	488.90	0.1154	0.0003
463.07	0.0215	0.0002	476.98	0.0540	-0.0004	490.90	0.1318	0.0018
465.06	0.0252	0.0007	479.01	0.0615	-0.0005	492.89	0.1482	0.0017
467.05	0.0275	-0.0006	480.96	0.0704	0.0002			
469.04	0.0315	-0.0006	482.95	0.0796	0.0000			
				[C_6C_1im][Ntf_2]				
465.33	0.0227	0.0003	475.35	0.0448	0.0000	485.38	0.0853	-0.0011
467.33	0.0262	0.0004	477.35	0.0509	-0.0003	487.35	0.0996	0.0017
469.33	0.0299	0.0002	479.36	0.0582	-0.0003	489.37	0.1137	0.0026
471.35	0.0337	-0.0004	481.36	0.0663	-0.0004			
473.34	0.0384	-0.0007	483.37	0.0748	-0.0011			
				[C_7C_1im][Ntf_2]				
464.95	0.0174	0.0000	474.86	0.0352	0.0002	484.85	0.0680	-0.0006
466.94	0.0200	-0.0001	476.82	0.0402	0.0001	486.90	0.0786	0.0003
468.93	0.0232	0.0001	478.88	0.0458	-0.0003	488.88	0.0894	0.0004
470.86	0.0263	-0.0002	480.83	0.0522	-0.0004	490.89	0.1014	0.0002
472.88	0.0310	0.0005	482.81	0.0595	-0.0005	492.88	0.1152	0.0005
				[C_8C_1im][Ntf_2]				
473.10	0.0229	0.0003	481.08	0.0397	0.0006	489.09	0.0665	0.0004
475.08	0.0257	-0.0003	483.27	0.0451	-0.0001	491.08	0.0757	0.0006
477.10	0.0293	-0.0005	485.08	0.0511	0.0002	493.08	0.0852	0.0000
479.10	0.0341	-0.0001	487.08	0.0580	-0.0001	495.09	0.0955	-0.0012
				[$C_{10}C_1$im][Ntf_2]				
479.37	0.0214	0.0001	485.36	0.0325	-0.0001	491.37	0.0492	0.0000
481.35	0.0245	-0.0001	487.36	0.0374	0.0000	493.38	0.0564	0.0001
483.35	0.0285	0.0002	489.39	0.0428	-0.0002	495.38	0.0645	0.0002
				[$C_{12}C_1$im][Ntf_2]				
480.89	0.0154	-0.0001	486.84	0.0239	0.0001	492.81	0.0362	0.0000
482.87	0.0180	0.0001	488.94	0.0276	0.0000			
484.85	0.0206	0.0000	490.81	0.0314	-0.0001			

$\Delta p = p - p_{calc}$, where p_{calc} is calculated from the Clarke and Glew equation (eq. 5) with the parameters given in Table 1.

Estimation of the $\Delta_l^g C_{p,m}^o$ for the ionic liquids studied:

The heat capacities in the gaseous phase, $C_{p,m}^o(g)$, for [C_2mim][NTf_2], [C_4mim][NTf_2], [C_6mim][NTf_2] and [C_8mim][NTf_2], were calculated by Paulechka *et al.*[1] by quantum chemical calculations using B3LYP/6-31+G(2df,p) level of theory. The heat capacities in the liquid phase, $C_{p,m}^o(l)$, for the mentioned IL, were determined via adiabatic calorimetry, by the same research group.[2-4] The values of $\Delta_l^g C_{p,m}^o$ were estimated considering the same temperature for all ILs, T = 388 K. Therefore, the values of $\Delta_l^g C_{p,m}^o(T = 388\ K)$ for the other ILs ([C_3mim][NTf_2], [C_5mim][NTf_2], [C_7mim][NTf_2], [C_{10}mim][NTf_2] and [C_{12}mim][NTf_2]), were estimated using the linear fitted function ($\Delta_l^g C_{p,m}^o$ = -5.40 n(C) − 100.47) derived from fitting the literature data of $\Delta_l^g C_{p,m}^o(T = 388\ K)$ as a function of the cation alkyl chain length (Figure S1). The estimated values of $\Delta_l^g C_{p,m}^o(T = 388\ K)$ for the nine ionic liquids studied are presented in table S2.

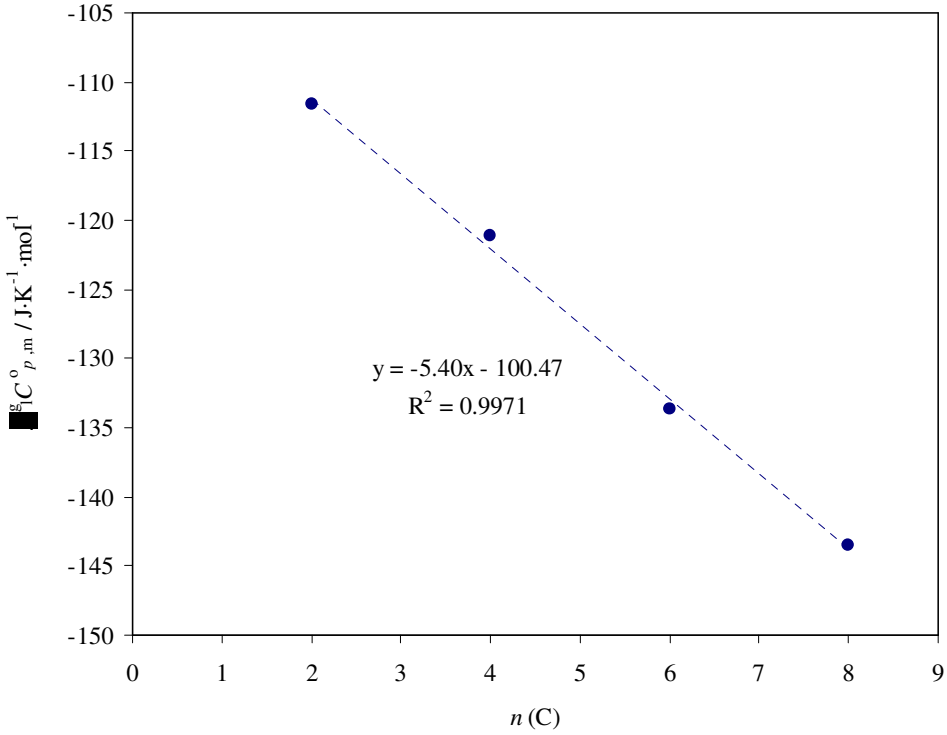

Figure S1 - lLiterature data of $\Delta_l^g C_{p,m}^o$ (T = 388 K) as a function of the cation alkyl chain length.

Table S2. Values of heat capacities in the gaseous and liquid phases available in literature and the calculated values of $\Delta_l^g C_{p,m}^o$ at T = 388 K.

Ionic Liquid	$C_{p,m}^o$ (l) / J·K^{-1}·mol^{-1}	$C_{p,m}^o$ (g) / J·K^{-1}·mol^{-1} (1)	$\Delta_l^g C_{p,m}^o$ (T = 388 K)* / J·K^{-1}·mol^{-1}
[C_2mim][NTf_2]	548.7 [3]	437.1	-112
[C_3mim][NTf_2]	-	-	-117 [a]
[C_4mim][NTf_2]	617.1 [4]	496.0	-121
[C_5mim][NTf_2]	-	-	-127 [a]
[C_6mim][NTf_2]	689.3 [2]	555.6	-134
[C_7mim][NTf_2]	-	-	-138 [a]
[C_8mim][NTf_2]	759.9 [3]	616.5	-143
[C_{10}mim][NTf_2]	-	-	-154 [a]
[C_{12}mim][NTf_2]	-	-	-165 [a]

[a] $\Delta_l^g C_{p,m}^o$ (388 K) estimated using the linear fitted function ($\Delta_l^g C_{p,m}^o$ = -5.40 n(C) - 100.47) derived from fitting of the literature data of $\Delta_l^g C_{p,m}^o$ (388 K) as a function of the cation alkyl chain length. * Uncertainty was set as 5 J·K^{-1}·mol^{-1}.

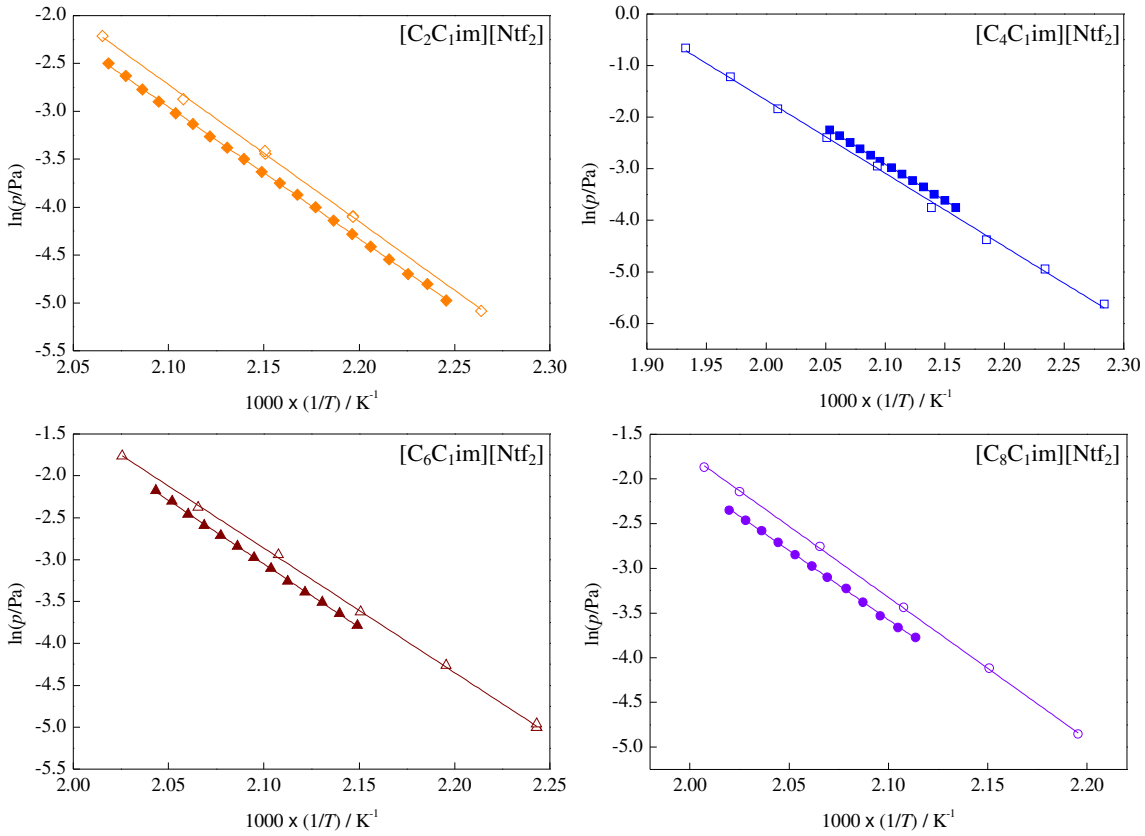

Figure S2. Plots of ln(p/Pa) = f [(1/T)/K^{-1}] for the values obtained in this work and those by Zaitsau *et al.*[5]. [C_2C_1im][Ntf_2]: ◆ - this work, ◇- Zaitsau *et al*; [C_4C_1im][Ntf_2]: ■ - this work, □- Zaitsau *et al.*; [C_6C_1im][Ntf_2]: ▲ - this work, △- Zaitsau *et al.*; [C_8C_1im][Ntf_2]: ● - this work, ○- Zaitsau *et al.*.

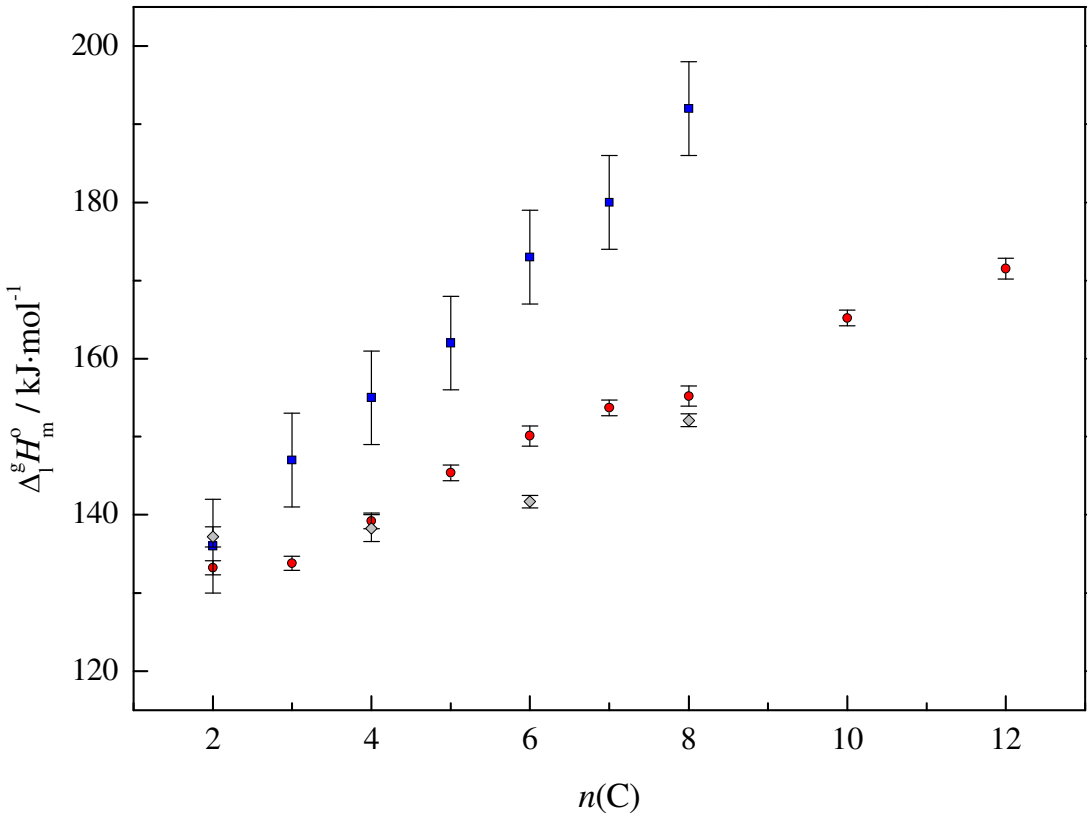

Figure S3. Comparison of the standard molar enthalpies of vaporization, at T=298.15 K, in comparison with the literature. ● - This work (Knudsen effusion / Quartz crystal microbalance method); ■ - Santos *et al.* (Calvet microcalorimetry)[6]; ◇ - Zaitsau *et al.* (Knudsen effusion method)[5].

Absolute standard molar entropies in gaseous and liquid phases:

Table S3. Values of standard molar entropies of vaporization and the absolute standard molar entropies in gaseous and liquid phases at reference temperature, T = 298.15 K. SI

Ionic Liquid	$\Delta_l^g S_m^o$ / J·K^{-1}·mol^{-1}	S_m^o(g) / J·K^{-1}·mol^{-1}	S_m^o(l) / J·K^{-1}·mol^{-1}
$[C_2C_1im][Ntf_2]$	170.0 ± 2.6	777.9 *	607.9
$[C_3C_1im][Ntf_2]$	173.4 ± 2.8	814.9[a]	641.5
$[C_4C_1im][Ntf_2]$	183.8 ± 2.6	853.8 *	670.0
$[C_5C_1im][Ntf_2]$	196.9 ± 2.8	893.0[a]	696.1
$[C_6C_1im][Ntf_2]$	206.9 ± 4.0	926.2 *	719.3
$[C_7C_1im][Ntf_2]$	213.0 ± 2.4	971.0[a]	758.0
$[C_8C_1im][Ntf_2]$	214.0 ± 3.7	1014.0 *	800.0
$[C_{10}C_1im][Ntf_2]$	231.8 ± 2.8	1088.2[a]	856.4
$[C_{12}C_1im][Ntf_2]$	242.5 ± 3.5	1166.2[a]	923.7

* reference [1];

[a] S_m^o(g) , at T = 298.15 K, calculated using the the linear fitted function (S_m^o(g) = 39.035 n(C) + 697.8)derived from fitting of the literature data of S_m^o(g) as a function of the cation alkyl chain length.

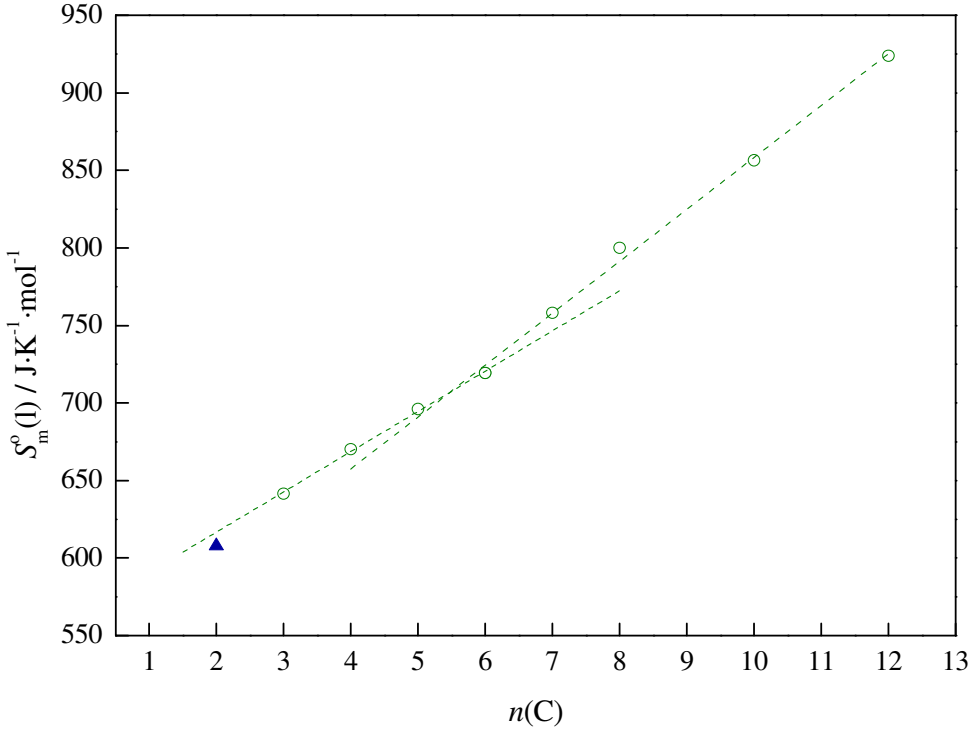

Figure S4 - Absolute standard molar entropies in liquid phase, at (T=298.15 K), as a function of the number of carbon atoms in the alkyl side chain of the cation, n(C).

Molecular Dynamics

Ionic liquids based on $[Ntf_2]^-$ exhibit particularly low viscosity, a fact attributable to the flexibility of the anion. This issue has been investigated by various authors[1,7] who have confirmed that $[Ntf_2]^-$ can exist as different interconvertible conformational isomers both as isolated ions or as constituents of ionic pairs in the gas phase or condensed ions in ionic liquids. The alkyl side chain of $[C_nC_1im]^+$ ions with n>1, can also exhibit distinct conformations, namely different preferred dihedral angles around the CR-N-C1-C2 (planar or non-planar conformations) and N-C1-C2-C3 (gauche or trans conformations) bonds.[8] The combination of these two types of flexible ions in the $[C_nC_1im][Ntf_2]$ series yields ionic liquids whose structure and energetics are dominated by complex potential energy surfaces[1,9], a fact which can explain the different trends found for the vaporization properties. The .character of $[C_2C_1im][Ntf_2]$ relative to the rest of the $[C_nC_1im][Ntf_2]$ series and the corresponding $\Delta_l^g H_m^o$ [n(C)] and $\Delta_l^g S_m^o$ [n(C)] gata presented in figures 3 and 4 can be interpreted in terms of structural modifications occurring both in the condensed and vapor phases as n(C) changes from 2 to 3. In this case the main structural alteration occurs around the CR-N-C1-C2 dihedral. Whereas in the $[C_2C_1im]^+$ cation the planar isomer represents a stable configuration (local energy minimum), in the $[C_2C_1im]^+$ and all other $[C_nC_1im]^+$ cations, the planar isomer is just a transition state. This state of affairs (observed spectroscopically[8] and corroborated by ab initio calculation[1,8,9] and molecular dynamics simulations[9]) can be observed in figure S5, which compares the distribution of conformational isomers in the condensed phase of $[C_2C_1im][Ntf_2]$ and $[C_4C_1im][Ntf_2]$. The central (red) peak corresponding to stable planar conformers in $[C_2C_1im][Ntf_2]$ is replaced by a flat region corresponding to transition states between the two non-planar conformers of $[C_4C_1im][Ntf_2]$. In other

words, only in the case of $[C_2C_1im]^+$ is it possible for (short) alkyl side chain to remain in a coplanar position with the ring. From $[C_3C_1im]^+$ onwards, the alkyl side chain (the C2 carbon) atom will begin either above or below the aromatic plane, facilitating inter-conversion between the two states. It is hard to estimate the effect of this obvious structural modification on the vaporization process. As it is an intramolecular change that can occur in both the condensed and vapor phases, the net effect may be quite small. However one can infer that the enhanced flexibility of the alkyl side chain at the C2 carbon due to the substitution of the planar peak by an interconversion plateau when one goes from $[C_2C_1im][Ntf_2]$ to $[C_3C_1im][Ntf_2]$ will ease interaction between the ions in the condensed phase. The peak/plateau substitution also indicates the possibility of a more entropic condensed phase of $[C_3C_1im][Ntf_2]$ relative to that of $[C_2C_1im][Ntf_2]$. In spite of the limitation to two stable conformers in the former ionic liquid and three in the latter, the number of intermediate transitional forms is enhanced in $[C_3C_1im][Ntf_2]$.

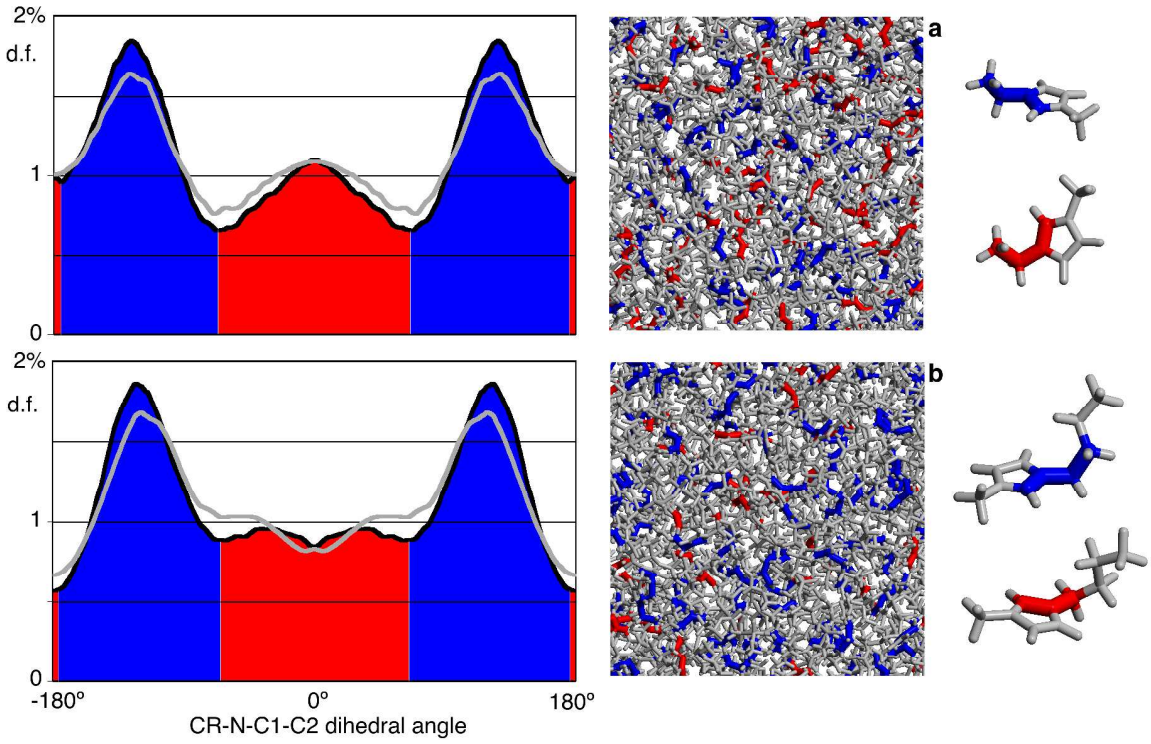

Figure S5. Probability distribution function (d.f.) of the conformational isomers of $[C_2C_1im]^+$ (top) and $[C_4C_1im]^+$ (bottom) around the CR-N-C1-C2 dihedral angle. The red and blue codes refer to isomers with planar (red) or non-planar (blue) conformations. The two snapshots are of simulated condensed phases of $[C_2C_1im][Ntf_2]$ and $[C_4C_1im][Ntf_2]$ used to calculate the distribution functions. Snapshot (b) reveals a prevalence of non-planar (blue) conformers relative to snapshot (a). The black and gray lines correspond to simulation runs performed at 303 and 343 K, respectively.

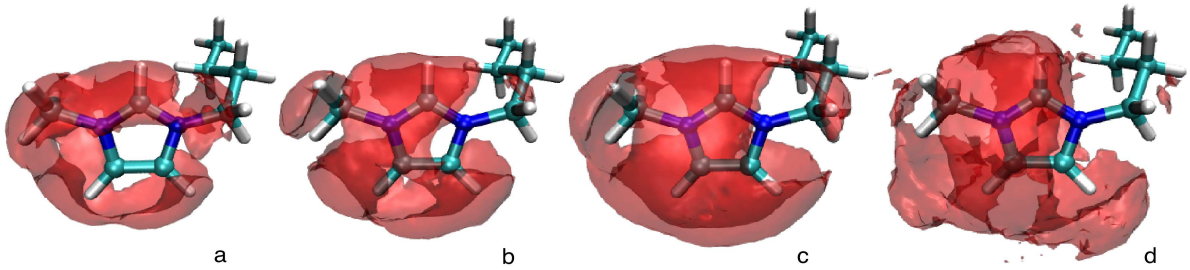

Figure S6. Spatial distribution functions of the anion center-of-mass around the $[C_4C_1im]^+$cation in the condensed phase of different $[C_4C_1im][X]$ ionic liquids. The anion size (indicated between parentheses as effective molar volumes in $cm^3 \cdot mol^{-1}$ at 298 K)[10] increases from left to right: (a) Cl^-(25.9); (b) $[BF_4]^-$ (53.4); (c) $[PF_6]^-$(73.7); (d) $[Ntf_2]^-$ (158.7).

Viscosity Data for $[C_nmim][NTf_2]$

The viscosity data available in the literature[11] was fitted using Vogel–Fulcher–Tammann (VFT) (equation 1),

$$\eta = A \times e^{B/(T-Tg)} \qquad (1)$$

where *A*, *B* and *C* are fitting parameters. Table S4, lists the fitting coefficients and the activation energy of viscosity, $\left[\frac{\partial \ln(\eta)}{\partial(1/T)}\right]$, for the ionic liquids studied in this work. [11]

Table S4. Fitting coefficients of VFT equation and the activation energy for the viscosity data available in the literature.[11]

Ionic Liquid	*A* /mPa.s	*B*	*C* / K	*E* /kJ·mol^{-1}
$[C_2mim][NTf_2]$	0.22810	692.5	158.9	26.40
$[C_3mim][NTf_2]$	0.19660	713.7	167.2	30.76
$[C_4mim][NTf_2]$	0.14880	794.7	161.8	31.59
$[C_5mim][NTf_2]$	0.12630	838.2	161.3	33.08
$[C_6mim][NTf_2]$	0.12540	855.9	163.0	34.63
$[C_7mim][NTf_2]$	0.11680	888.1	162.4	35.62
$[C_8mim][NTf_2]$	0.09972	943.3	160.2	36.64
$[C_9mim][NTf_2]$	0.09534	971	159.8	37.49
$[C_{10}mim][NTf_2]$	0.08095	1028	157.4	38.35
$[C_{12}mim][NTf_2]$	0.08497	1040	159.6	40.04

References:

(1) Paulechka, Y. U.; Kabo, G. J.; Emel'yanenko, V. N. *J. Phys. Chem. B* **2008**, *112*, 15708–15717.

(2) Blokhin, A. V.; Paulechka, Y. U.; Kabo, G. J. *J. Chem. Eng. Data* **2006**, *51*, 1377–1388.

(3) Paulechka, Y. U.; Blokhin, A. V.; Kabo, G. J.; Strechan, A. A. *J. Chem. Thermodynamics* **2007**, *39*, 866–877.

(4) Blokhin, A. V.; Paulechka, Y. U.; Strechan, A. A.; Kabo, G. J. *J. Phys. Chem. B* **2008**, *112*, 4357–4364.

(5) Zaitsau, D. H.; Kabo, G. J.; Strechan, A. A.; Paulechka, Y. U.; Tschersich, A.; Verevkin, S. P.; Heintz, A. *J. Phys. Chem. A* **2006**, *110*, 7303-7306.

(6) Santos, L. M. N. B. F.; Canongia Lopes, J. N.; Coutinho, J. A. P.; Esperança, J. M. S. S.; Gomes, L. R.; Marrucho, I. M.; Rebelo, L. P. N. *J. Am. Chem. Soc.* **2007**, *129*, 284-285.

(7) Canongia Lopes, J. N.; Shimizu, K.; Pádua, A. A. H.; Umebayashi, Y.; Fukuda, S.; Fujii, K.; Ishiguro, S.-i. *J. Phys. Chem. B* **2008**, *112*, 1465-1472.

(8) Umebayashi, Y.; Fujimori, T.; Sukizaki, T.; Asada, M.; Fujii, K.; Kanzaki, R.; Ishiguro, S.-i. *J. Phys. Chem. A* **2005**, *109*, 8976-8982.

(9) Canongia Lopes, J. N.; Pádua, A. A. H. *J. Phys. Chem. B* **2006**, *110*, 7485-7489.

(10) Rebelo, L. P. N.; Canongia Lopes, J. N.; Esperança, J. M. S. S.; Guedes, H. J. R.; Łachwa, J.; Najdanovic-Visak, V.; Visak, Z. P. *Acc. Chem. Res*. **2007**, *40*, 1114–1121.

(11) Tariq, M.; Carvalho, P. J.; Coutinho, J. A.P.; Marrucho, I. M.; Canongia Lopes, J. N.; Rebelo, L. P.N. *Fluid Phase Equilibria* **2011**, *301*, 22–32.